

GmTIR1/GmAFB3-based auxin perception regulated by miR393 modulates soybean nodulation

Zhaoming Cai^{1,2*}, Youning Wang^{1*}, Lin Zhu¹, Yingping Tian³, Liang Chen³, Zhengxi Sun^{3,4}, Ihteram Ullah^{1,3} and Xia Li¹

¹State Key Laboratory of Agricultural Microbiology, College of Plant Science and Technology, Huazhong Agricultural University, Wuhan 430070, China; ²College of Life Science and Technology, Yangtze Normal University, Chongqing 408100, China; ³Center for Agricultural Resources Research, Institute of Genetics and Developmental Biology, Chinese Academy of Sciences, 286 Huaizhong Road, Shijiazhuang, Hebei 050021, China; ⁴University of Chinese Academy of Sciences, Beijing 100049, China

Author for correspondence:

Xia Li

Tel: +86 027 87856638

Email: xli@mail.hzau.edu.cn

Received: 16 January 2017

Accepted: 9 April 2017

New Phytologist (2017) **215**: 672–686

doi: 10.1111/nph.14632

Key words: auxin, *Glycine max* (Soybean), GmTIR1/AFB3, miR393, nodule number, rhizobial infection.

Summary

- Auxins play important roles in the nodulation of legumes. However, the mechanism by which auxin signaling regulates root nodulation is largely unknown. In particular, the role of auxin receptors and their regulation in determinate nodule development remains elusive.
- We checked the expression pattern of the auxin receptor *GmTIR1/GmAFB3* genes in soybean. We analyzed the functions of *GmTIR1/AFB3* in the regulation of rhizobial infection and nodule number, and also tested the functions of miR393 during nodulation and its relationship with *GmTIR1/AFB3*.
- The results showed that *GmTIR1* and *GmAFB3* genes exhibit diverse expression patterns during nodulation and overexpression of *GmTIR1* genes significantly increased infection foci and eventual nodule number. *GmTIR1/AFB3* genes were post-transcriptionally cleaved by miR393 family and knock-down of the miR393 family members significantly increased rhizobial infection and the nodule number. Overexpression of the mutated form of *GmTIR1C* at the miR393 cleavage site that is resistant to miR393 cleavage led to a further increase in the number of infection foci and nodules, suggesting that miR393s modulate nodulation by directly targeting *GmTIR1C*.
- This study demonstrated that GmTIR1- and GmAFB3-mediated auxin signaling, that is spatio-temporally regulated by miR393, plays a crucial role in determinate nodule development in soybean.

Introduction

Legumes are high nitrogen (N)-demanding plant species. To meet the high demand for N, legumes have evolved a specialized lateral root organ, the root nodule, which hosts nitrogen-fixing bacteria to convert the atmospheric N₂ into NH₃ that can be utilized by plants under low nitrate conditions. In exchange, legume plants provide carbohydrates and energy for growth and survival of N-fixing rhizobia (Desbrosses & Stougaard, 2011; Downie, 2014). Thus, the symbiotic nodule is a unique lateral root organ conducting activities for the mutual benefit of plants and rhizobia. Despite the complexity, nodule development can be divided into four successive stages: dedifferentiation of cortical cells of roots, nodule primordia formation, nodule emergence, and formation of functional nodules (Ferguson *et al.*, 2010).

Nodule development in legumes is determined by soil nitrate conditions and interaction with symbiotic rhizobia. Under low nitrate conditions, nodulation is triggered by Nod factors secreted by rhizobia, and the interplay between rhizobia and

plant developmental regulatory signaling pathways results in dedifferentiation of cortical cells and subsequent formation of *de novo* nodules in roots (Streeter, 1985; Reid *et al.*, 2010). Phytohormone auxins are essential regulators in legume nodulation. Changes in auxin concentrations were associated with nodule formation in the model legume plant *Lotus japonicus* that generates determinate nodules (Suzaki *et al.*, 2012). Localized auxin accumulation in cortical cells of various leguminous roots has shown to be associated with nodule initiation by physiological and genetic approaches (Hirsch *et al.*, 1989; Wasson *et al.*, 2006). Gene expression analysis results indicated that PIN-mediated auxin efflux is involved in auxin distribution during nodulation (Saňko-Sawczenko *et al.*, 2016). A very recent study showed that application of auxin influx inhibitors and knockout of the functional ortholog (MtLAX2) of Arabidopsis Auxin transporter protein 1 (AUX1) reduced nodulation of *Medicago truncatula*, demonstrating that auxin influx is required for nodulation (Roy *et al.*, 2017). Furthermore, expression patterns of numerous auxin-inducible markers were changed at various developmental stages of nodule development (Suzaki *et al.*, 2012; Turner *et al.*, 2013), indicating an essential role of the auxin signaling and

*These authors contributed equally to this work.

cellular auxin responses during nodule initiation, primordia development and nodule organogenesis. Recent genetic evidence reveals that perception of Nod factors by root epidermal cells somehow activates the cytokinin signaling pathway in the cortex of the infected roots, which then induces a key transcription factor NODULE INCEPTION that positively regulates local auxin accumulation in some cortical cells to trigger cortical cell dedifferentiation and cell division, leading up to nodule primordia development (Plet *et al.*, 2011; Suzaki *et al.*, 2012; Held *et al.*, 2014). Auxin accumulation is also negatively controlled by the autoregulation of nodulation (AON) to suppress further nodule formation (van Noorden *et al.*, 2006; Suzaki *et al.*, 2012). Loss-of-functions in the *SUNN* (*Super Numeric Nodules*) and *HAR1* (*Hypernodulation Aberrant Root formation 1*) gene encoding the nodule auto-regulation receptor-like kinase in *M. truncatula* and *L. japonicus* resulted in increased auxin transport from shoot to root and ectopic auxin accumulation in roots is associated with the supernodulation phenotype (van Noorden *et al.*, 2006; Suzaki *et al.*, 2012). Therefore, auxin distribution and auxin maxima in the infected legume roots are regulated precisely.

Despite progress in the role of auxin accumulation during nodule early development, relatively little is known about the regulatory role of auxin signaling in nodulation. Recent reports showed that overexpression of miR160 and miR167 repressed gene expression of a set of auxin response factors, altered root sensitivity to auxin, and altered nodule numbers in soybean (Turner *et al.*, 2013; Wang *et al.*, 2015), confirming that the downstream auxin signaling components are involved in nodule development. However, overexpression of soybean miR393(a) that is supposed to target the auxin receptor and repress their mRNAs/proteins, did not affect nodulation of soybean although sensitivity to auxin was reduced (Turner *et al.*, 2013). Interestingly, overexpression of miR393 in *M. truncatula* significantly changed the nodule development (Mao *et al.*, 2013). Thus, it is proposed that the auxin TIR1/AFB receptor-mediated signaling pathway may play a minimal role in determinate nodule development, and the miR393-auxin receptor modules regulate indeterminate but not determinate nodule development (Mao *et al.*, 2013; Turner *et al.*, 2013). Until now, direct evidence concerning the function of the TIR1/AFB auxin receptors in soybean nodule formation and organogenesis is lacking.

In order to further define the functions of the auxin signaling in soybean nodulation, we have systematically analyzed the roles of auxin receptors genes and their upstream regulators miR393s in rhizobial infection and nodule development. Here we have shown that the miR393-GmTIR1/AFB3 module-mediated auxin perception and auxin response play an important role in rhizobial infection and nodule development in soybean.

Materials and Methods

Plant and rhizobia growth conditions

Soybean (*Glycine max* (L.) Merrill cv Williams 82) was used to clone the miRNAs and target genes, for 5'-RACE, and in the functional analysis of miR393 and its targets. The plant growth

conditions and inoculation procedure using *Bradyrhizobium japonicum* strain USDA110 were modified from Wang *et al.* (2009). Briefly, we suspended the bacteria with low-nitrogen (N) nutrient solution, and inoculated 30 ml diluted bacteria for each seedling. For RNA extraction, plant roots were rinsed briefly in PBS buffer (pH 7.5) to remove vermiculite and perlite particles. Harvested tissues were frozen immediately in liquid N and stored at -80°C until used for RNA extraction.

Soybean hairy root transformation and *B. japonicum* inoculation assay

Soybean transformation to generate hairy root composite plants was done using *Agrobacterium rhizogenes* K599 according to methods described previously (Kereszt *et al.*, 2007; Jian *et al.*, 2009). For nodulation assays, transgenic composite plants were transplanted to pots (10 × 10 cm) containing a mixture of 3 : 1 vermiculite and perlite, which was irrigated with a N-deficient solution as described by Wang *et al.* (2009). The plants were grown for 1 wk (16 h of light, 25°C and 50% relative humidity) to allow recovery. The plants were then inoculated with a suspension of *B. japonicum* strain USDA110 ($\text{OD}_{600} = 0.08$). At 28 d post-inoculation (dpi), nodules were assayed and the roots were harvested to study relative gene expression.

RNA extraction and quantitative PCR analysis

Total RNA was extracted from leaves, roots and nodules using Trizol reagent (Tiagen Biotech (Beijing) Co. Ltd, Beijing, China). Total RNA samples were treated with DNase I (Invitrogen) to remove contaminating genomic DNA. First-strand cDNA was synthesized from the total RNA using a FastQuant RT Kit (Tiagen Biotech (Beijing) Co. Ltd). Quantitative polymerase chain reactions (qPCR) were performed using SuperReal PreMix Plus (SYBR Green; Tiagen Biotech (Beijing) Co. Ltd) using gene-specific primers (Supporting Information Table S1) for the genes analyzed. *GmELF1B* was used as the internal reference gene (Jian *et al.*, 2008).

Vector construction

For the promoter analysis, putative promoter regions of *miR393d* (1873 bp), *GmTIR1A* (989 bp), *GmTIR1B* (2002 bp), *GmTIR1C* (1643 bp), *GmTIR1D* (1587 bp), *GmAFB3A* (1864 bp) and *GmAFB3B* (1101 bp) were amplified from Williams 82 genomic DNA and inserted into the vector pCAMBIA 1391. The following restriction enzymes were used: *Bam*HI and *Bgl*II for *miR393d*:*GUS* construction; *Hind*III and *Bam*HI for *GmTIR1C*:*GUS* and *GmAFB3A*:*GUS* construction; *Xba*I for *GmTIR1A*:*GUS*, *GmTIR1B*:*GUS* and *GmTIR1D*:*GUS* construction; and *Bam*HI for *GmAFB3A*:*GUS* and *GmAFB3B*:*GUS* construction. For the *miR393d* overexpression construct, the sequence containing pre-miRNA fragment of *miR393d* (645 bp) was amplified and inserted into the plant expression vector pTF101.1 under the control of the *CaMV35S* promoter using the restriction enzymes *Xba*I and *Sac*I. To reduce the activity of miR393, the *MIM393*

under the control of *CaMV35S* promoter in pTF101.1 vector was also made using the restriction enzymes *Xba*I and *Sac*I, as described by Todesco *et al.* (2010). For the overexpression construct of *GmTIR1/GmAFB3* fused with GFP, the *GmTIR1A*, *GmTIR1C* and *GmAFB3A* coding sequences were amplified and inserted into the plant expression vector pTF101-GFP using the restriction enzymes *Sma*I and *Bam*HI under the control of the *CaMV35S* promoter. For site-directed mutagenesis, four point mutations in the miRNA-binding sites of *GmTIR1A*, *GmTIR1C* and *GmAFB3A* mRNAs were designed according to the procedure of Parry *et al.* (2009). All primers used for plasmid construction are listed in Table S1.

Curled root hair statistical assays

In order to examine the infection events, the root segments (4-cm) of hairy roots below the hypocotyl–root junctions of the composite transgenic plants were cut and harvested at 6 dpi and then rinsed briefly in sterile PBS buffer to remove vermiculite/perlite particles. The root fragments were then stained with 0.01% methylene blue for 15 min and washed three times with deionized water as described previously (Subramanian *et al.*, 2004). The stained transgenic roots were observed with an Olympus CX31 biological microscope for infection events. The number of root hairs forming tight curls were counted and were referred to as ‘Curled Root Hair’ ($n = 10–12$).

Statistical analysis

All data were analyzed using SIGMAPLOT 10.0 (Systat Software, Inc., Chicago, IL, USA) and GraphPad PRISM 5 (GraphPad Software Inc., La Jolla, CA, USA) software. The averages and standard deviations of all results were calculated. Student’s *t*-tests were performed to generate *P*-values for two groups of samples comparison, and for multiple groups of samples, the one-way ANOVA followed by the Dunnett test was used for *P*-value generation between Empty vector and each transgenic lines. Student’s Newman–Kuels test was used for the comparison among multiple groups of data.

Results

GmTIR1 and *GmAFB3* auxin receptor genes have multiple members

In Arabidopsis, *TIR1/AFB* genes are major auxin receptors in plant growth regulation and AFB3 is a central receptor mediating lateral root growth in response to N (Vidal *et al.*, 2013). To investigate whether TIR1 and AFB3 family receptors mediate auxin response in soybean nodulation, we searched the soybean genome to identify the Arabidopsis *TIR1* and *AFB3* orthologs in soybean. Four *GmTIR1* (*Glyma.02G152800*, *Glyma.10G021500*, *Glyma.19G206800* and *Glyma.03G209400*) and two *GmAFB3* (*Glyma.19G100200* and *Glyma.16G050500*) auxin receptor genes were identified (Fig. S1a,b). Similar to Arabidopsis *TIR1*, the predicted sequences of the four *GmTIR1* genes contain three exons and two introns and the predicted open reading frames

coding sequences encode proteins with 585, 585, 587 and 586 amino acids, respectively (Figs S1c, S2a). These proteins showed high sequence identity to Arabidopsis TIR1 (Table S2), and each contains several LRR (leucine-rich repeat) domains and one F-BOX domain (Fig. S2a). Based on the phylogenetic analysis of proteins, the four *GmTIR1* genes were named as *GmTIR1A*, *GmTIR1B*, *GmTIR1C* and *GmTIR1D* that are divided into two subgroups (Fig. S3).

A similar bioinformatics analysis showed that the two *GmAFB3* genes have similar gene structures to Arabidopsis *AFB3* and the sequences of the *GmAFB3* genes have three exons and two introns (Fig. S1c). Both proteins were composed of 572 amino acids and the sequence identity of the GmAFB3 proteins to Arabidopsis AFB3 was > 74% (Fig. S2b; Table S2). Based on the clustering pattern of GmAFB3 proteins with the Arabidopsis AFB3, the soybean *AFB3* genes were named as *GmAFB3A* and *GmAFB3B* (Fig. S3).

In order to confirm that the *GmTIR1* genes are the ortholog of *AtTIR1* but not other Arabidopsis auxin receptors, we further analyzed the orthology relationship among all the auxin receptor F-BOX family members including *AtAFB1*, *AtAFB2*, *AtAFB3*, *AtAFB4* and *AtAFB5* using online Integrative Orthology Viewer (http://bioinformatics.psb.ugent.be/plaza/versions/plaza_v3_dicos/). The integrative orthology analysis showed that the four *GmTIR1* genes were indeed the ortholog of *AtTIR1* but not other genes (Fig. S4). Similar analysis was also conducted for *GmAFB3* genes, and the result showed that the *GmAFB3* genes were also the orthologs of *AtAFB3* but not other auxin-signaling F-BOX family genes (Fig. S4).

GmTIR1/AFB3 positively regulate soybean nodulation

In order to investigate whether the soybean putative auxin receptor genes affect root nodule formation, we constructed an RNAi vector designed to repress all the *GmTIR1/AFB3* gene family members by choosing a 267-bp sequence of *GmTIR1C*, more than 97% of the sequence was conserved among the *GmTIR1/AFB3* genes. We then transformed the vector into soybean hairy roots to analyze the nodulation phenotypes of the composite transgenic plants at the rhizobial infection and nodule maturation stages. qPCR analysis showed that the average transcript expression levels of all the six genes in *GmTIR1/AFB3* knock-down lines were significantly reduced compared with the vector control lines (Fig. 1a). Intriguingly, we found that the number of curled root hairs was dramatically reduced at 6 dpi with *B. japonicum* strain USDA110 (Fig. 1b–d). In the vector control roots, the average number of curled root hairs was 29.1 per root segment; by contrast, the average number in the *GmTIR1/AFB3* knock-down roots was only 14.4 (Fig. 1d). We also counted the nodule numbers of the *GmTIR1/AFB3* knock-down roots and the empty vector control roots at 28 dpi. The result showed that the average nodule number of the RNAi-*GmTIR1/AFB3* lines was significantly reduced compared with the empty vector control lines (Fig. 1e–g). The RNAi-*GmTIR1/AFB3* lines produced *c.* 42% fewer root nodules per hairy root (3.8 ± 1.07) than the vector control (9.1 ± 1.21).

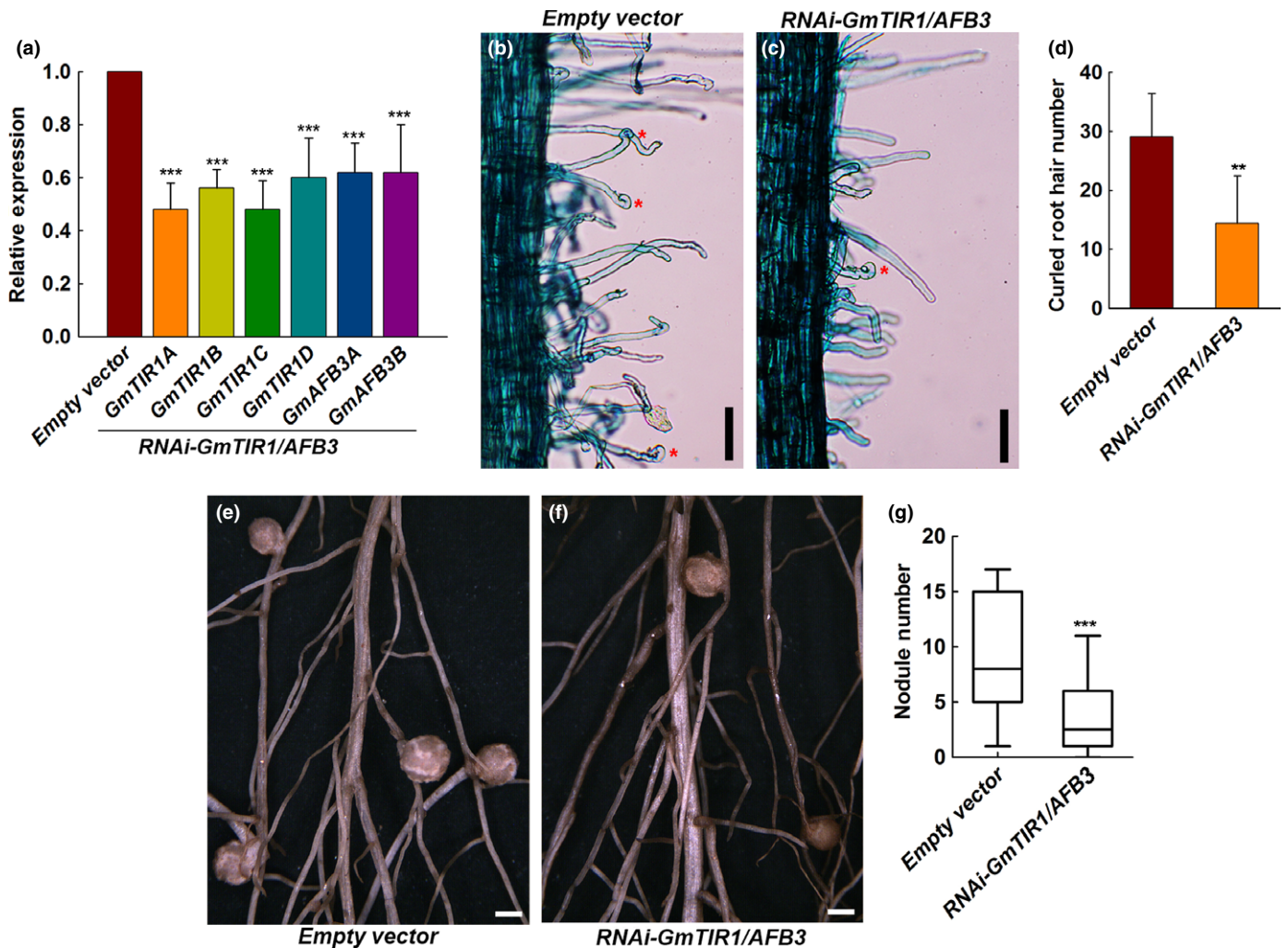


Fig. 1 The auxin receptors *GmTIR1/AFB3* positively regulate nodulation in soybean. (a) Expression levels of *GmTIR1A*, *GmTIR1B*, *GmTIR1C*, *GmTIR1D*, *GmAFB3A* and *GmAFB3B* in the *RNAi-GmTIR1/AFB3* transgenic hairy roots, the gene expression levels were expressed as mean transcript values \pm SD in all the transgenic lines and were normalized against the geometric mean of the soybean reference gene *GmELF1B*. (b–d) Curled root hair number of the empty vector control and *RNAi-GmTIR1/AFB3* transgenic hairy roots. The asterisk marks the curled root hair (b, c), and the curled root hair number was expressed as mean values \pm SD in all of the transgenic lines (d). Bars: (b, c) 50 μ m. (e–g) Nodule number phenotypes of the empty vector control and *RNAi-GmTIR1/AFB3* transgenic hairy roots. (e, f, the image data, bars, 2 mm; g, the quantitative data). Box plots show the distribution of nodule numbers per root. The boxes indicate data within the first and third quartiles, and the thick black line indicates the median). One-way ANOVA followed by the Dunnett test was used for (a), and each bar was compared with the empty vector. Student's *t*-test was used for significant difference analyses for (d, g). Significant difference: **, $P < 0.01$; ***, $P < 0.001$.

GmTIR1 and *GmAFB3* family members show different expression patterns during nodule development

In order to further test whether *GmTIR1* and *GmAFB3* mediate nodulation, we analyzed the expression patterns of all the *GmTIR1* and *GmAFB3* genes during nodule development by generating the transgenic hairy roots expressing four *GmTIR1pro:GUS* and two *GmAFB3pro:GUS*. First, we analyzed the expression patterns of these genes in noninoculated roots. As shown in Fig. 2, *GmTIR1A*, *GmTIR1B* and *GmAFB3A* were expressed at high levels in main roots, lateral root primordia and lateral roots (Fig. S5a,b,e,g,h,k,m,n,q). Both *GmTIR1A* and *GmAFB3A* were expressed strongly in main root tips and lateral root primordia (Fig. S5a,c,g,k,m,q). *GmTIR1C* and *GmTIR1D* displayed

tissue-specific expression patterns. *GmTIR1C* was expressed specifically in the meristem zone of the root, including the meristem tissue of the main root and lateral root, as well as lateral root primordium (Fig. S5c,i,o), and *GmTIR1D* was specifically expressed in the root tips of the main root and lateral root, as well as lateral root primordia (Fig. S5d,j,p). In sharp contrast, *GmAFB3B* expression was hardly detectable in the root (Fig. S5f,l,r). We then analyzed the expression patterns of the genes during nodulation. GUS staining results showed that the *GmTIR1* and *GmAFB3* family genes exhibited diverse expression patterns during nodulation. Among the *GmTIR1* genes, *GmTIR1A* and *GmTIR1B* showed a similar expression pattern: they were strongly expressed in both roots and nodules at the early stage of nodule development. The levels of *GmTIR1A* and *GmTIR1B*

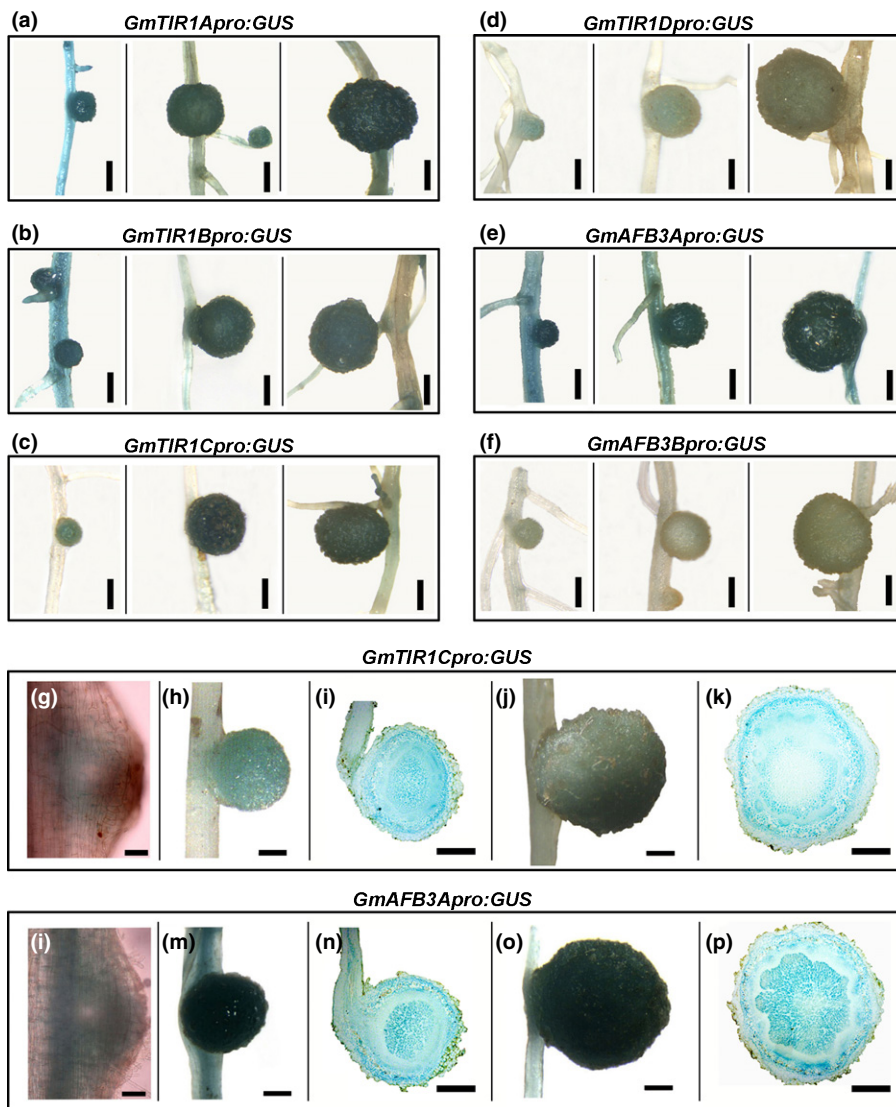


Fig. 2 The expression pattern of auxin receptors *GmTIR1* and *GmAFB3* family genes. (a–f) Histochemical staining of *GmTIR1pro:GUS* and *GmAFB3pro:GUS* in the roots and nodules of soybean at 10, 14 and 28 d post-inoculation (dpi) with rhizobia. (a) *GmTIR1Apro:GUS*; (b) *GmTIR1Bpro:GUS*; (c) *GmTIR1Cpro:GUS*; (d) *GmTIR1Dpro:GUS*; (e) *GmAFB3Apro:GUS*; (f) *GmAFB3Bpro:GUS*. Bars, 1 mm. (g–k) Histochemical staining of *GmTIR1Cpro:GUS* at 7 dpi (g), 14 dpi (h, i) and 28 dpi (j, k). (l–p) Histochemical staining of *GmAFB3Apro:GUS* at 7 dpi (l), 14 dpi (m, n) and 28 dpi (o, p). Bars: (g, l) 100 µm; (h–k, m–p) 500 µm.

expression maintained at high levels in developing nodules, whereas their expression levels were substantially reduced in roots with developing nodules (Fig. 2a,b). By contrast, a distinct expression pattern was observed for *GmTIR1C* and *GmTIR1D*: both genes were expressed predominantly in young and developing nodules, and nearly no expression was observed in the roots with nodules (Fig. 2c,d). *GmAFB3A* was expressed at high levels in both root and nodules during nodule development, whereas *GmAFB3B* was expressed at extremely low levels in roots and nodules (Fig. 2e,f).

In order to examine the expression patterns of the genes at the tissue levels in developing nodules, we chose *GmTIR1C* and *GmAFB3A* that represent two distinct patterns in two groups of auxin receptors genes for further study. Transverse section analysis results showed that *GmTIR1C* and *GmAFB3A* exhibited distinct expression patterns during nodule formation and nodule organogenesis. During nodule primordia formation, *GmTIR1C* was expressed mainly in the cells forming nodule primordia but not in other peripheral cells (Fig. 2g). In young nodules,

GmTIR1C was expressed in the nodule cortex and N-fixation zone of nodules; upon nodule maturation, the overall *GmTIR1C* expression was not altered (Fig. 2h–k). *GmAFB3A* was expressed in all of the cells of nodule primordia together with root tissues during nodule primordia formation (Fig. 2l). During nodule development, *GmAFB3A* exhibited a similar expression pattern to *GmTIR1C* in young nodules and mature nodules of soybean plants, and with the exception of its high level of expression in roots (Fig. 2m–p).

GmTIR1A and *GmTIR1C* play major roles in soybean nodulation

In order to further examine the roles of the individual *GmTIR1/GmAFB3* genes in soybean nodulation, we selected the genes that represent three types of expression patterns and phylogenetically distinct subgroups of *GmTIR1* and *GmAFB3* genes. *GmTIR1A* and *GmTIR1C* were placed in the *GmTIR1* group and *GmAFB3A* was kept in the *GmAFB3* subgroup for further

functional analyses. First, we performed qPCR to analyze the expression patterns of *GmTIR1A*, *GmTIR1C* and *GmAFB3A* genes during rhizobia inoculation and nodule development (Fig. S6a–i). The transcript levels of *GmTIR1A* and *GmAFB3A* genes were not affected by *B. japonicum* USDA110 inoculation within 24 h (Fig. S6a,c), but *GmTIR1C* expression was upregulated at 12 h post-inoculation (hpi) (Fig. S6b). The expression level of *GmTIR1A* was not greatly altered in the roots at 10 and 28 dpi and uninfected control, and *GmAFB3A* was decreased dramatically in the roots at 28 dpi compared with that at 10 dpi (Fig. S6d,f). Interestingly, *GmTIR1C* showed an increased expression level in the roots at both 10 and 28 dpi compared to control (Fig. S6e). We also measured the expression of the *GmTIR1A*, *GmTIR1C* and *GmAFB3A* in nodules. All of the tested genes except *GmTIR1A* were expressed in the young and mature nodules at a relatively constant levels (Fig. S6g–i).

Next, we generated the transgenic hairy roots overexpressing *GmTIR1A*, *GmTIR1C* and *GmAFB3A* under the control of *CaMV35S* promoter, and evaluated the number of nodules at 28 dpi with *B. japonicum* strain USDA110. To identify the transgenic hairy roots, we conducted a two-step analysis to discriminate the transformed hairy roots from nontransformed roots: PCR analysis of the *Bar* gene in the used vector and then qPCR

of the target gene expression in the *Bar* positive roots. Only the hairy roots that were *Bar*-positive and exhibited significantly increased expression levels of the target genes were used for subsequent phenotype analysis (Fig. S7a–d). As shown in Fig. 3(a–e), overexpression of *GmTIR1A* and *GmTIR1C* significantly increased the number of nodules per hairy root. Unexpectedly, the transgenic roots overexpressing *GmAFB3A* under the control of the *CaMV35S* promoter produced a comparable number of nodules as the vector control hairy roots at 28 dpi (Figs 3a,b,f, S7e,f). These results suggest that *GmTIR1A* and *GmTIR1C* play important roles for soybean nodulation, whereas *GmAFB3A* may play a minor role in this process.

The *GmTIR1* and *GmAFB3* genes were responsive to auxin in soybean

Because *GmTIR1* and *GmAFB3* proteins are putative orthologs of Arabidopsis *TIR1* and *AFB3*, we speculated that these proteins regulate nodulation through modulation of cellular response to auxin. To test the possibility, we analyzed expression of the *GmTIR1A*, *GmTIR1C* and *GmAFB3A* genes in response to auxin. Nine-day-old seedlings were treated with 1 μ M 2,4-D and qPCR was used to test the *GmTIR1A*,

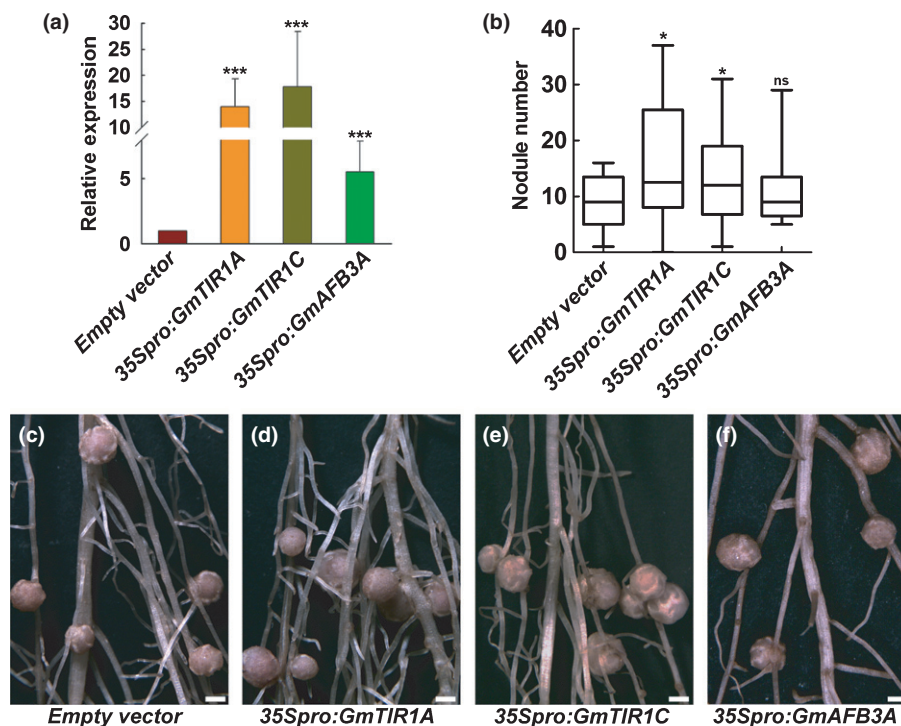


Fig. 3 The auxin receptors *GmTIR1* positively regulate nodulation in soybean. (a) Expression levels of *GmTIR1A*, *GmTIR1C* and *GmAFB3A* in the *35Spro:GmTIR1A*, *35Spro:GmTIR1C* and *35Spro:GmAFB3A* transgenic hairy roots, respectively. The gene expression levels were expressed as mean transcript values \pm SD in all the transgenic lines and were normalized against the geometric mean of the soybean reference gene *GmELF1B*. (b–f) Phenotypic analysis of soybean nodulation at 28 d post-inoculation (dpi). (b) Quantitative data. Box plots show the distribution of nodule numbers per root. The boxes indicate data within the first and third quartiles, and the thick black line indicates the median. (c–f) Image data for the empty vector control (c) and the transgenic roots overexpressing *GmTIR1A* (d), *GmTIR1C* (e) and *GmAFB3A* (f). Three independent biological repeats were performed, and in total 20, 24, 30 and 24 transgenic hairy roots of the empty vector, *35Spro:GmTIR1A*, *35Spro:GmTIR1C* and *35Spro:GmAFB3A* were used, respectively. The one-way ANOVA followed by the Dunnett test was used for significant difference analysis, and each bar was compared with the empty vector. Significant differences: *, $P < 0.05$; ***, $P < 0.001$; ns, not significant. Bars, 2 mm.

GmTIR1C and *GmAFB3A* gene expression in roots at the specified time points. The results showed that the expression of *GmTIR1A* remained quite stable within 24 h, whereas *GmTIR1C* expression was increased at 12 h after 2,4-D treatment and remained elevated after 24 h (Fig. S8a,b). By contrast, *GmAFB3A* was significantly induced by auxin starting from 6 h after 2, 4-D treatment and maintained at the higher levels (Fig. S8c). We also checked the expression levels of *GmTIR1A*, *GmTIR1C* and *GmAFB3A* genes in the seedlings treated with 2,4-D for 3 d as a long-term auxin treatment (Fig. 4a–c). Notably, all three genes were markedly upregulated in the treated roots compared with the control (Fig. 4a–c).

The *GmTIR1A*, *GmTIR1C* and *GmAFB3A* genes are the direct targets of soybean miR393

In *Arabidopsis*, the *TIR1/AFB* family genes are directly targeted by miR393 (Parry *et al.*, 2009). To test whether the *GmTIR1A*, *GmTIR1C* and *GmAFB3A* genes are also the direct targets of miR393 in soybean, we first performed a bioinformatics analysis to search the complementary sequences in these genes. The result showed that *GmTIR1A*, *GmTIR1C* and *GmAFB3A* genes contain a single complementary sequence to miR393 miRNAs in the third exon (Fig. S9). We then conducted the RNA ligase-mediated 5' Rapid Amplification of cDNA Ends (RLM-5'RACE) assay to validate the prediction. As shown in Fig. S9, the mRNAs of the *GmTIR1A*, *GmTIR1C* and *GmAFB3A* genes were cleaved at the typical miRNA cleavage sites of the complementary sequences between the 10th to 11th nucleotides from the 5' end of miR393. These results confirmed that *GmTIR1A*, *GmTIR1C* and *GmAFB3A* genes are indeed the targets of miR393 in soybean.

miR393 family members are differentially expressed in soybean nodulation

In order to better understand the role of miR393 in soybean nodulation, we first performed the phylogenetic analysis of the miR393 family using their precursor sequences in soybean. As shown in Fig. 5(a), the soybean miR393 family contains 11 members and can be divided into two groups (<http://mirbase.org/>) and each group contains two subgroups of miR393 miRNAs.

When comparing the mature sequences, miR393a represents a single type of miRNA containing 21 nucleotides, whereas miR393c/d/e/f/g and miR393h/i/j/k share the exact same sequence with miR393a but containing one additional nucleotide 'C' and 'U' at their 3' and 5' termini, respectively (Table S3). Notably, miR393b found in the miRBase differed greatly in its mature sequence from the other family members and, thus, miR393b was excluded from this study.

Next, we analyzed the expression patterns of three types of mature miR393s during nodule development in soybean. Stem-loop qPCR analyses showed that all the miR393 miRNAs were expressed at fairly low levels in the uninoculated roots of 9-d-old seedlings, and among them, miR393a and miR393h/i/j/k were expressed at higher levels than miR393c/d/e/f/g (Fig. 5b). Upon rhizobia inoculation, the expression of miR393a and miR393h/i/j/k were slightly reduced at 6 hpi and then increased at 12 hpi, whereas miR393c/d/e/f/g showed more severe reduction at 6 hpi and maintained at lower levels at 12 hpi (Figs 5c, S10a,d). During nodule development, the expression of miR393a and miR393h/i/j/k was upregulated and remained unchanged in the inoculated roots, respectively; by contrast, miR393c/d/e/f/g were downregulated at 10 dpi and then upregulated at 28 dpi in the inoculated roots (Figs 5d, S10b,e). miR393a, miR393c/d/e/f/g and miR393h/i/j/k also showed different expression patterns during nodule development. In young nodules, three groups of miR393 were expressed at very low levels, yet their expression levels were elevated substantially at 28 dpi, although miR393a and miR393h/i/j/k expression were much higher than miR393c/d/e/f/g (Figs 5e, S10c,f).

miR393d directly targets auxin receptor genes

Previous studies have shown that *miR393a* do not affect soybean nodule development and that miR393j-3p was involved in soybean nodulation through targeting *ENOD93* but not auxin receptors (Mao *et al.*, 2013; Turner *et al.*, 2013; Yan *et al.*, 2015). Therefore, we speculated that the miR393c/d/e/f/g showing a different expression pattern during nodulation may be the upstream regulators of auxin receptor genes, such as *GmTIR1C* in nodulation regulation. Thereafter, we chose to concentrate our research

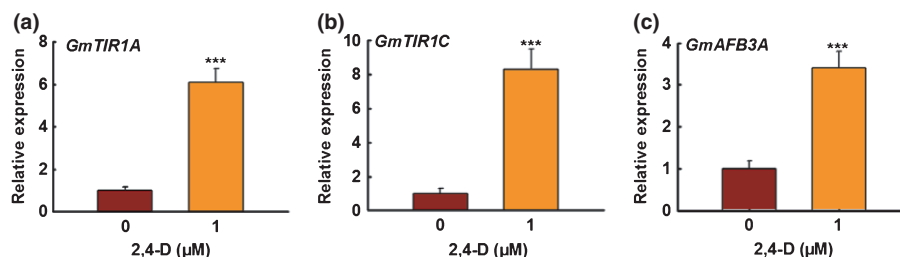


Fig. 4 The expression of *GmTIR1A*, *GmTIR1C* and *GmAFB3A* were induced by 2, 4-D treatment in soybean roots. Nine-day-old seedlings after germination were treated with solutions without or with 1 μM 2,4-D, and the roots were collected for RNA extraction. Quantitative polymerase chain reaction analysis of *GmTIR1A*, *GmTIR1C* and *GmAFB3A* expression was performed after treatment for 3 d. The gene expression levels were expressed as mean transcript values ± SD of three independent biological repeats. The *GmELF1B* was used as an internal control. Student's *t*-test was used for the significant difference analysis: ***, $P < 0.001$.

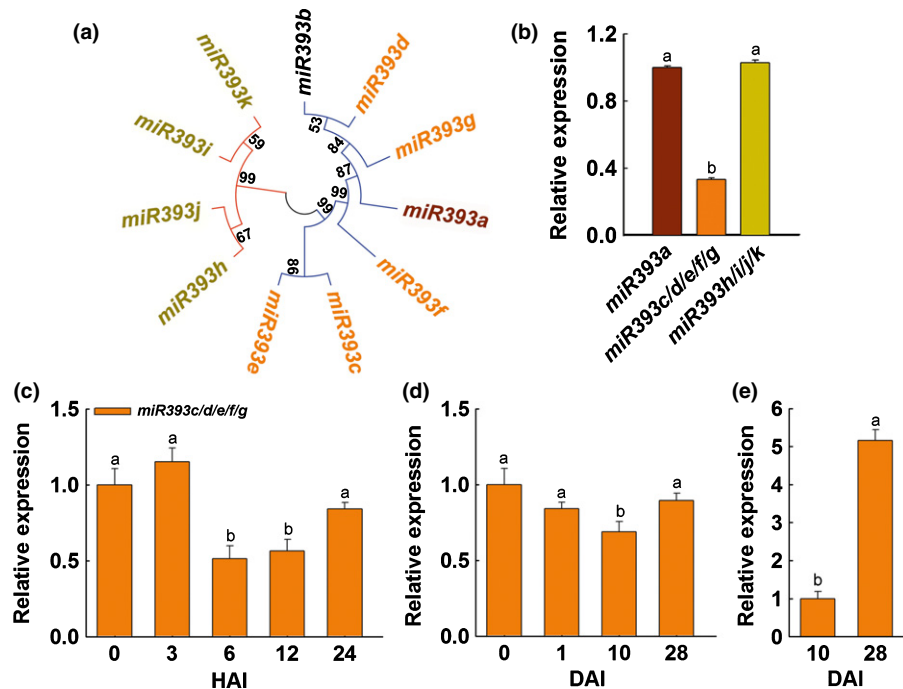


Fig. 5 Phylogenetic and expression analysis of soybean miR393 family genes. (a) Phylogenetic analysis of the precursor sequences of miR393 family members. The pre-miRNA sequences of the miR393 family member were used for the alignment, and the phylogenetic neighbor-joining tree was constructed using MEGA5 phylogenetic analysis software. (b) Expression of three groups of miR393 family members in roots before *Bradyrhizobium japonicum* inoculation. (c) Expression of miR393c/d/e/f/g family members in roots at the indicated hours post-inoculation (hpi) with *B. japonicum*. (d) Expression levels of miR393c/d/e/f/g in roots at the indicated days post-inoculation (dpi) during nodule development. (e) Expression of miR393c/d/e/f/g in young and mature nodules at 10 and 28 dpi. The gene expression levels were expressed as mean transcript values \pm SD of three independent biological repeats and were normalized against the geometric mean of the soybean reference gene miR1520d. Different letters indicate a significant difference (Student–Newman–Kuels (SNK) test, $P < 0.05$).

on *miR393d*, a randomly selected member of the group miR393c/d/e/f/g.

In order to prove that *miR393d* is able to repress *GmTIR1C* expression *in vivo*, we made the constructs (*CaMV35Spro:GmTIR1C-GFP* and *CaMV35Spro:miR393d* precursor) and transiently expressed them by infiltrating the genes into *Nicotiana benthamiana* leaf cells. As shown in Fig. 6, the GFP fluorescence was strongly detected in the nuclei of *N. benthamiana* leaf cells when infiltrated with the *GmTIR1C-GFP* alone (Figs 6a, S11); By contrast, the intensity of the GFP fluorescence was reduced substantially when *CaMV35Spro:GmTIR1C-GFP* and *CaMV35Spro:miR393d* were coexpressed. The Western blot analysis of GmTIR1C-GFP protein proved that the amounts of the fusion protein in *N. benthamiana* leaves co-overexpressing miR393d and the target gene was reduced dramatically compared with that in the plant cells only overexpressing the target gene (Fig. 6b,c). To verify the result, we also coexpressed *miR393d* and *GmTIR1C* with four point mutations in the miR393 target site (*CaMV35Spro:mGmTIR1C-GFP*) in the *N. benthamiana* leaf cells (Fig. S12). As expected, overexpression of miR393 cannot repress the expression of *mGmTIR1C* (Fig. 6a–c). Using the same methods, we also proved that *GmTIR1A* and *GmAFB3A* were also negatively regulated by *miR393d* (Fig. S13a–f). Together, these results demonstrate that *miR393d* directly represses the expression of the target genes.

miR393d is specifically expressed in parenchyma cells during nodule development and negatively regulates the nodulation of soybean

In order to determine whether *miR393d* functionally targets auxin receptor genes, we sought to examine whether *miR393d* is expressed in a tissue-specific expression pattern. To this end, we assayed the expression of the *GUS* reporter gene in the *miR393dpro:GUS* transgenic hairy roots. As shown in Fig. 7(a), *GUS* activity was hardly detected in root cortical cells during nodule primordia formation at 7 dpi, but as nodules developed, weak *GUS* activity was observed in both roots and young nodules (Fig. 7b). Interestingly, strong expression of the *GUS* gene was observed in parenchyma cells between the N-fixation zone and cortex cells of 14-d-old nodules (Fig. 7c). When nodules became mature, the weak expression of *GUS* gene was mainly limited in the N-fixation zone of the 28-d-old nodules (Fig. 7d,e). Basically, *miR393d* showed tissue-specific expression patterns during nodule formation and nodule development, indicating a crucial role of miR393d during nodulation.

In order to test whether *miR393d* is indeed involved in nodulation regulation of soybean, we made the construct harboring *CaMV35Spro:miR393d* precursor and generated the transgenic roots overexpressing miR393d through *A. rhizogenes*-mediated

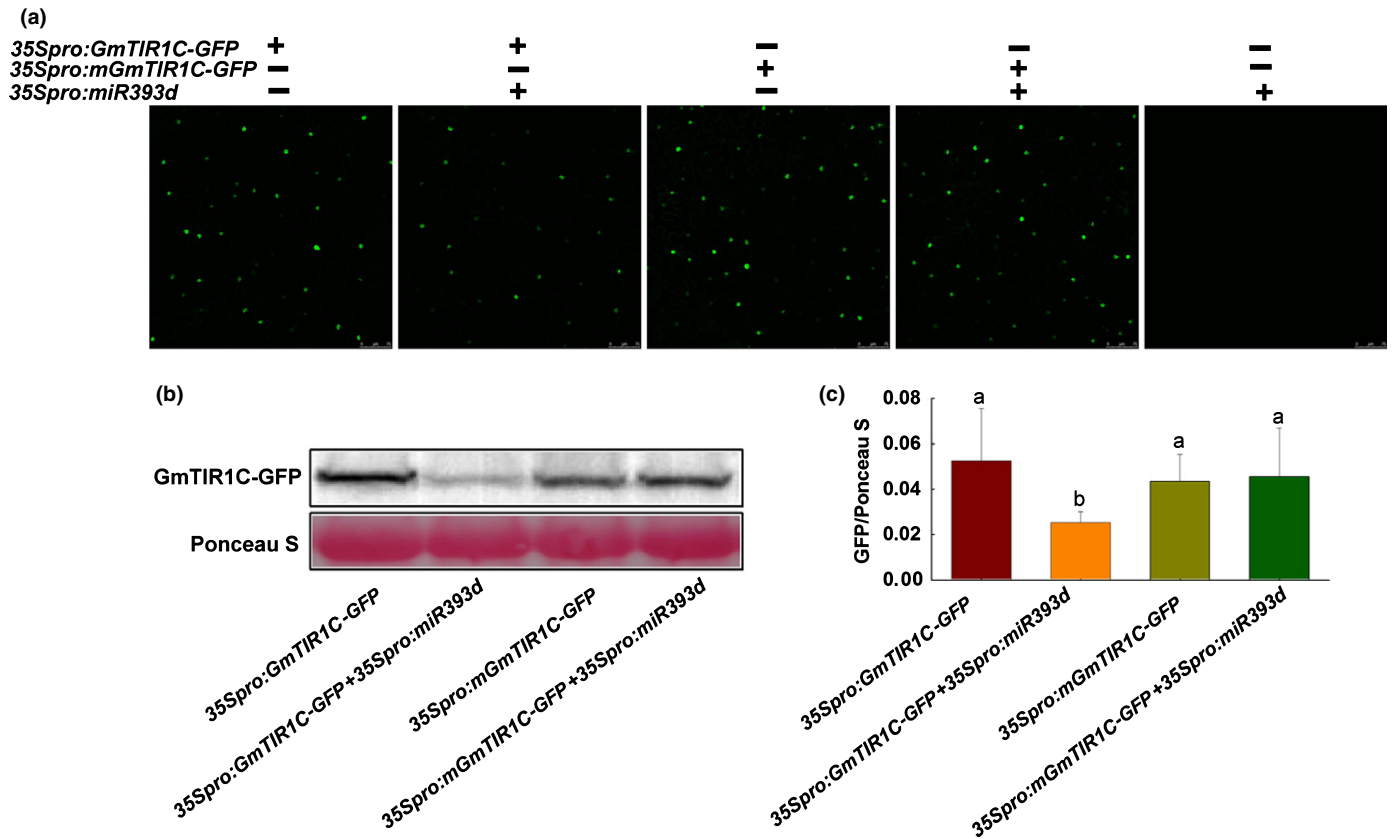


Fig. 6 *GmTIR1C* is repressed by miR393d. (a) Expression of *35Spro: GmTIR1C -GFP* or *35Spro:mGmTIR1C -GFP* and co-expression of them with *35Spro: miR393d* in *Nicotiana benthamiana*; GFP fluorescence was observed under confocal microscope. (b) Anti-GFP immunoblot analysis of *GmTIR1C-GFP* protein in the above samples. (c) The quantitative data of (b). Three independent biological repeats were performed with similar results, Ponceau S staining was used for loading control; error bars, + SD. Different letters indicate a significant difference (Student–Newman–Kuels (SNK) test, $P < 0.05$).

hairy root transformation. The hairy roots that overexpressed mature *miR393d* (Fig. 7f) were used for phenotypic analysis of the composite transgenic plants during nodulation including numbers of the curled root hairs and nodules. At 6 dpi, the curled root hair number in the *miR393d* overexpression roots was significantly reduced compared with that of the empty vector control roots (Fig. 7g,h,j). Accordingly, the number of nodules in transgenic roots overexpressing *miR393d* was significantly reduced compared with that of the roots expressing the empty vector, and the average number of nodules per *miR393d* overexpression root reduced markedly (Fig. 7k,l,n).

In order to demonstrate whether endogenous miR393d is required for nodulation, we attempted to see whether reduced miR393d affects nodule development. To do this, we made the construct expressing a target mimicry designed to hinder miR393 (MIM393) containing the short sequence mimicking the target site of miR393 (Fig. S14) and transformed the *CaMV35Spro: MIM393* into chimeric transgenic plants. qPCR results showed that the *CaMV35Spro:MIM393* was highly expressed (Fig. 7f). Phenotypic analyses of the *MIM393* transgenic composite plants showed that numbers of both the curled root hairs and nodules were dramatically increased (Fig. 7g,i,k,m,n). Together, these results demonstrate that miR393s act as negative regulators in soybean nodulation.

miR393d modulates nodulation through its effects on auxin receptors

In order to investigate whether *miR393d* is involved in soybean nodulation that is regulated by auxin receptor genes, we first tested the expression levels of *GmTIR1A*, *GmTIR1C* and *GmAFB3A* in the miR393d overexpression hairy root lines by qPCR. As shown in Fig. 8(a), the expression level of *GmTIR1C* and *GmAFB3A* in the miR393d overexpression roots were significantly reduced compared with those in the empty vector. However, we did not observe significant reduction in gene expression of *GmTIR1A*. We also tested the transcript levels of *GmTIR1A*, *GmTIR1C* and *GmAFB3A* in hairy roots successfully overexpressing the *MIM393* and found more than two-fold increases in *GmTIR1A*, *GmTIR1C* and *GmAFB3A* expression (Fig. 8b). The result suggests that miR393d may regulate nodule organogenesis by repressing the soybean auxin receptor target genes.

In order to prove the above prediction, we transformed the vector of *CaMV35Spro: GmTIR1C* together with its point mutation vector *CaMV35Spro:mGmTIR1C*, which is resistant to miR393 cleavage, to evaluate the nodule phenotypes. qPCR analysis showed that both *GmTIR1C* and its mutated form in the transgenic hairy roots was dramatically overexpressed at 28 dpi (Fig. 8c). Phenotypic analysis showed that *GmTIR1C*

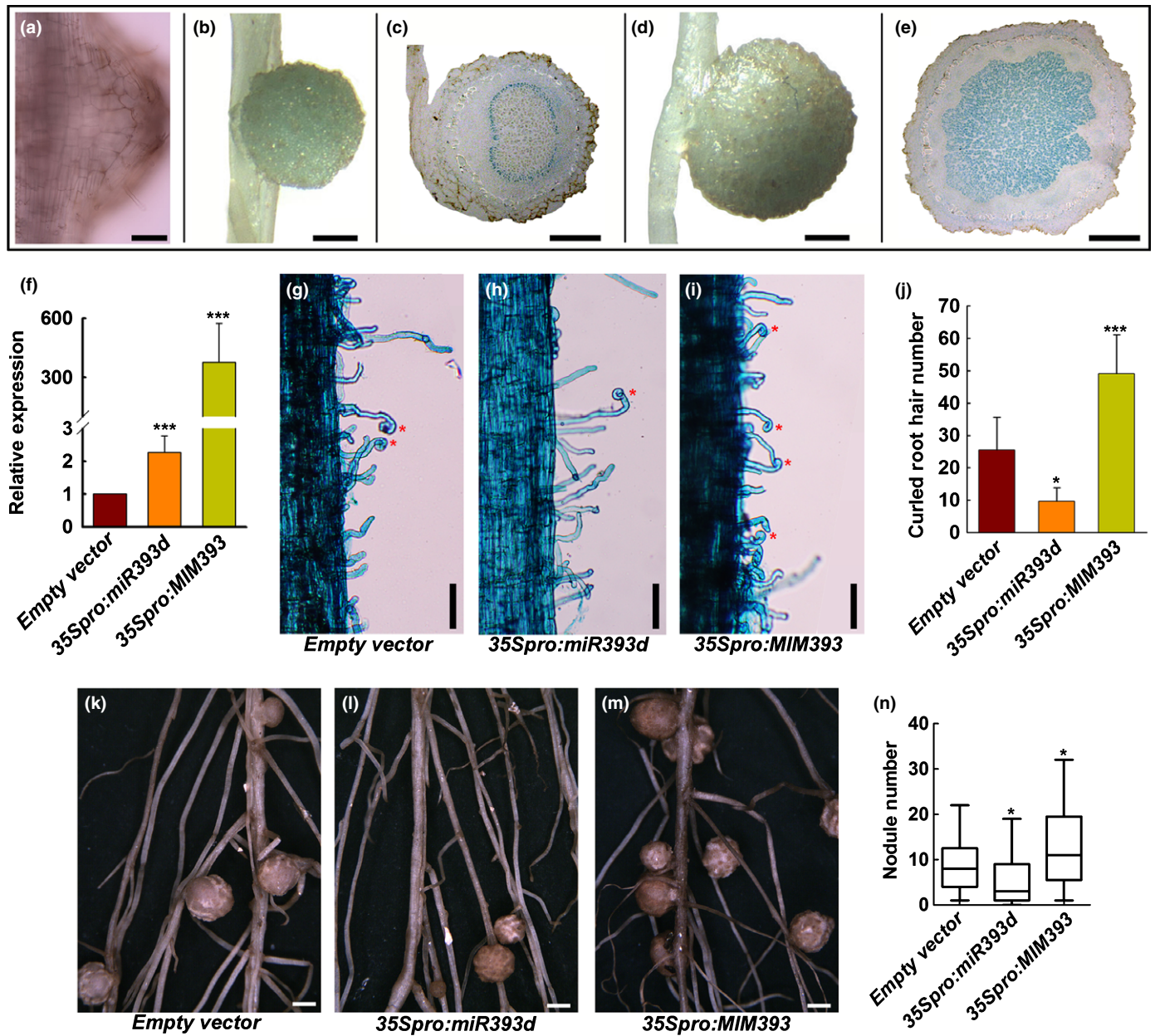


Fig. 7 The histochemical staining of *miR393dpro:GUS* and the nodulation phenotype of ectopic expression of miR393. (a–e) Histochemical staining of *miR393dpro:GUS*. (a) Nodule primordia at 7 DAJ. (b) The young nodule of 14 d post-inoculation (dpi). (c) Cross-section of nodule at 14 dpi. (d) The mature nodule of 28 dpi. (e) Cross-section of nodule at 28 DAJ. Bars: (a) 100 μ m; (b–e) 500 μ m. (f) Expression levels of mature *miR393d* and *MIM393* in the transgenic hairy roots expressing *35Spro:miR393d* and *35Spro: MIM393*, respectively. The gene expression levels were expressed as mean transcript values \pm SD in all the transgenic lines and were normalized against the geometric mean of the soybean reference gene *miR1520d* for *miR393d* and *GmELF1B* for *MIM393*, respectively. (g–i) The curled root hair number of the hairy root transformed with the empty vector, *35Spro:miR393d* and *35Spro: MIM393* at 6 dpi. The asterisk marks the curled root hair (g–i), the curled root hair number was expressed as mean values \pm SD in all the transgenic lines. Bars, 50 μ m. (k–n) The nodulation phenotypes of the hairy root transformed with the empty vector, *35Spro:miR393d* and *35Spro: MIM393* at 28 dpi. (k–m, the image data, bars, 2 mm. n, the quantitative data. Box plots show the distribution of nodule numbers per root. The boxes indicate data within the first and third quartiles, and the thick black line indicates the median). One-way ANOVA followed by the Dunnett test was used for the significant difference analysis, and each bar was compared with the empty vector. Significant differences: *, $P < 0.05$; ***, $P < 0.001$.

overexpression resulted in an increase in nodule number compared to the empty vector control, and strikingly, overexpression of *mGmTIR1C* led to a significantly greater increase in nodule number compared to vector control (Fig. 8d–g). The results suggest that miR393d regulates the nodulation by directly repressing the *GmTIR1C* gene.

GmTIR1/AFB3 regulates transcription levels of the auxin-responsive genes

In order to validate the role of miR393-*GmTIR1/AFB3*-mediated auxin signaling and auxin response in soybean nodulation, we analyzed the effects of *GmTIR1/AFB3* on

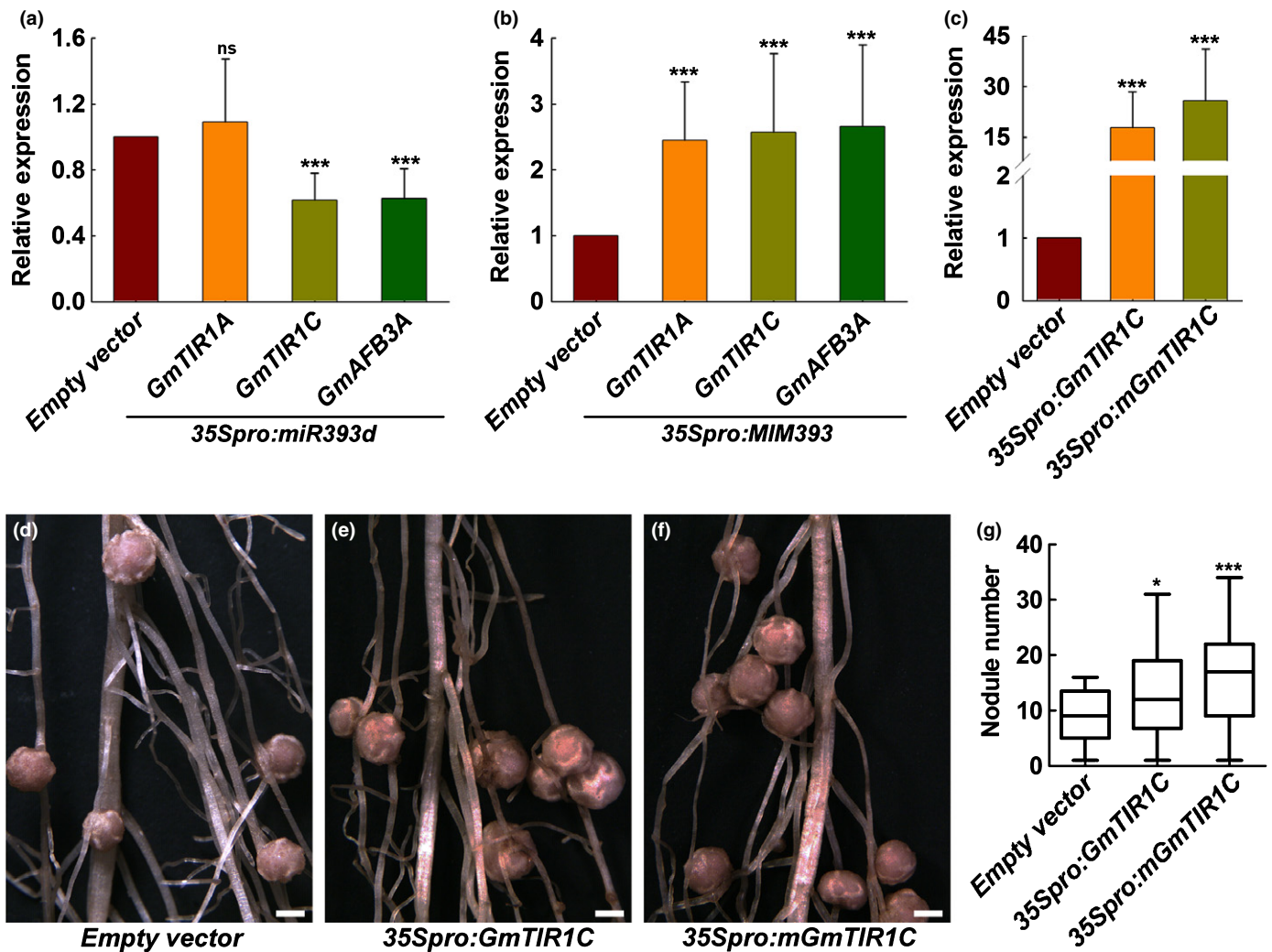


Fig. 8 miR393d modulates soybean nodule number by directly targeting *GmTIR1C*. (a, b) Quantitative polymerase chain reaction analysis of *GmTIR1A*, *GmTIR1C* and *GmAFB3A* expression in the hairy roots of *35Spro:miR393d* (a) and *35Spro:MIM393* (b); the empty vector was used as a control, and the gene expression levels were expressed as mean transcript values \pm SD in all the transgenic lines and were normalized against the geometric mean of the soybean reference gene *GmELF1B*. (c) Expression of *GmTIR1C* and the mutated form *mGmTIR1C* in the hairy roots overexpressing *GmTIR1C* and *mGmTIR1C*. The gene expression levels were expressed as mean transcript values \pm SD in all the transgenic lines and were normalized against the geometric mean of the soybean reference gene *GmELF1B*. (d–g) Phenotypic analysis of nodule numbers of the vector control, *35Spro:GmTIR1C* and *35Spro:mGmTIR1C* hairy roots (d–f, image data, bars, 2 mm; g, quantitative data). Box plots show the distribution of nodule numbers per root. The boxes indicate data within the first and third quartiles, and the thick black line indicates the median). Three independent biological repeats were performed, 30 and 27 transgenic hairy roots of *35Spro:GmTIR1C* and *35Spro:mGmTIR1C* were used for the nodule number analysis respectively. One-way ANOVA followed by the Dunnett test was used for the significant difference analysis, and each bar was compared with the empty vector. Significant differences: *, $P < 0.05$; ***, $P < 0.001$; ns, no significant difference.

transcription levels of *GmIAAs* (*GmIAA8*, *GmIAA9* and *GmIAA14*) and *GmARF8* (*GmARF8a* and *GmARF8b*) genes, which have been shown to mediate soybean nodulation (Turner *et al.*, 2013; Wang *et al.*, 2015). As shown in Fig. 9(a–c), the transcription levels of all the tested *GmIAA* genes were reduced significantly in the *GmTIR1/AFB3* knockdown hairy roots compared with those in the vector control roots; by contrast, the levels of *GmARF8a* and *GmARF8b* were dramatically elevated (Fig. 9d,e). This result confirms that *GmTIR1/AFB3C* modulates nodulation by regulating the cellular response to auxin in soybean.

Discussion

Auxin plays important roles in cellular responses and organogenesis *in plantae*. It has been shown that increased auxin response is associated with *de novo* organogenesis of nodules in legumes as indicated by the expression of the auxin-responsive marker genes, such as *DR5pro:GUS* and *GH3pro:GUS* in both indeterminate nodules (Mathesius *et al.*, 1998; Huo *et al.*, 2006; van Noorden *et al.*, 2007; Breakspear *et al.*, 2014) and determinate nodules (Pacios-Bras *et al.*, 2003; Takanashi *et al.*, 2011; Turner *et al.*, 2013). Later functional studies showed

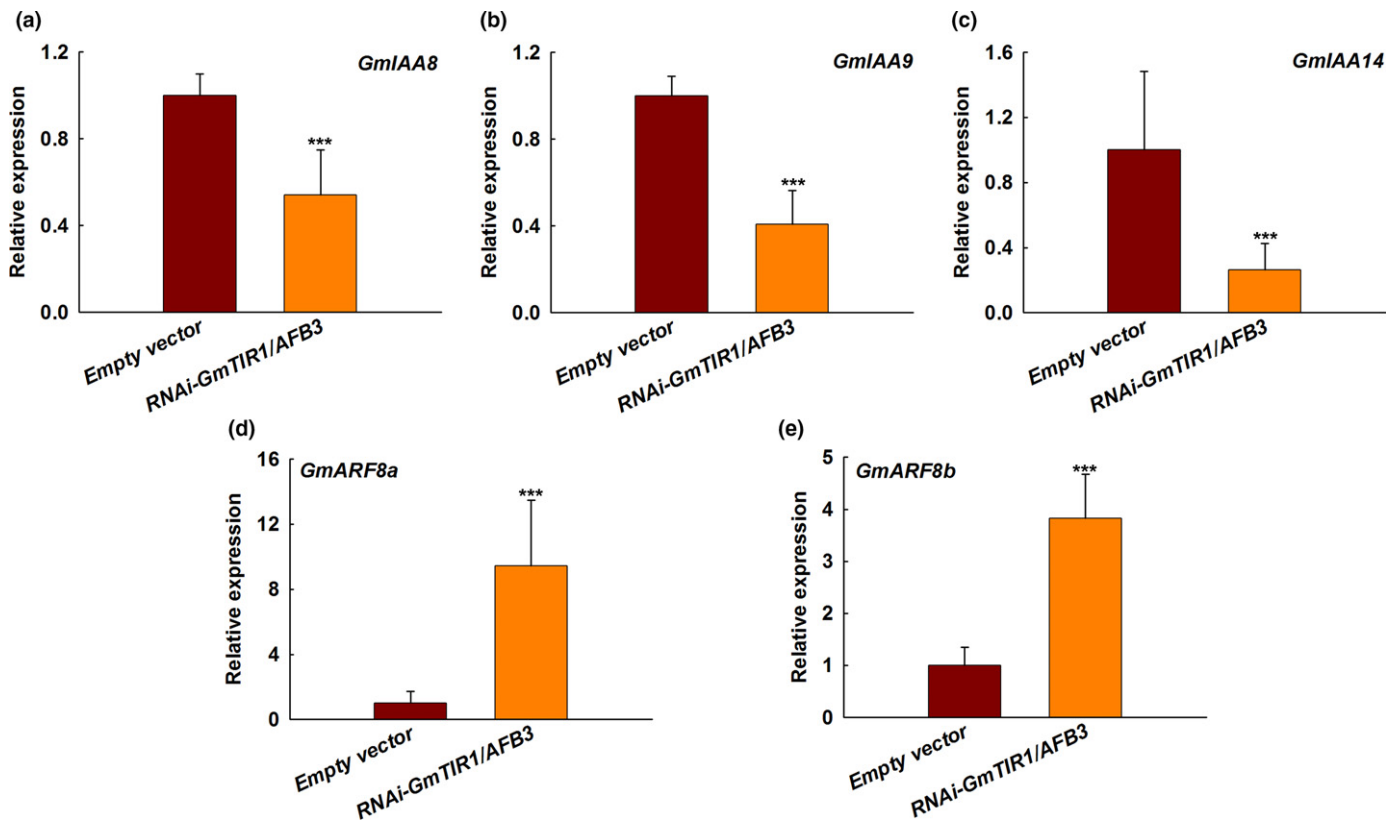


Fig. 9 The transcriptional levels of *GmIAA* genes and *GmARF8* in *GmTIR1/AFB3* knockdown transgenic hairy roots. Transcriptional levels of (a) *GmIAA8*, (b) *GmIAA9*, (c) *GmIAA14* and (d, e) *GmARF8a* and *GmARF8b*. The gene expression levels were expressed as mean transcript values \pm SD of three independent biological repeats and were normalized against the geometric mean of the soybean reference gene *GmELF1B*. Student's *t*-test was used for the significant difference analysis. Significant difference: ***, $P < 0.001$.

that manipulation of miR160 and miR167, which target the genes encoding auxin response factors (ARF), altered nodulation in soybean (Turner *et al.*, 2013; Wang *et al.*, 2015). Here, we provided direct evidence for the involvement of auxin signaling and responses in soybean nodulation. We showed that Arabidopsis *TIR1/AFB3* ortholog genes in soybean, that encode predicted auxin receptors, positively regulate rhizobial infection and nodule development. We also demonstrated that these soybean auxin receptor genes are direct targets of soybean miR393 during soybean nodulation.

The first step in auxin signaling is auxin-mediated activation of auxin receptors that interact with the transcriptional co-repressors (Aux/IAA) leading to Aux/IAA degradation (Tan *et al.*, 2007; Peer, 2013). Therefore, the concentrations of auxin receptors are crucial for the auxin signaling reaction. In Arabidopsis, there is only one copy of the *TIR1* and *AFB3* genes. Because soybean is an allotetraploid with at least two rounds of whole genome duplication, one can expect more than one copy of the *GmTIR1* and *GmAFB3* genes in soybean (Figs S1–S3). Our data supported the notion that these duplicated genes have redundant and/or diverged functions in soybean because all the genes of *GmTIR1* and *GmAFB3* were expressed differentially in roots and during nodule development (Figs 2, S5). For example, *GmTIR1A*, *GmTIR1B* and *GmAFB3A* were expressed at high levels in both roots and nodules at the early stage, *GmTIR1C* and

GmTIR1D were expressed mainly in lateral root primordia and nodules but not main roots, whereas *GmAFB3B* was expressed in both main roots and nodules. Based on the expression patterns of these genes, we speculate that the auxin receptor genes except for *GmAFB3B* may fine-tune root growth, lateral root formation, nodule initiation and nodule organogenesis, whereas *GmAFB3B* may be involved in shoot development. Because some auxin receptor genes were expressed in both roots and nodules, we do not exclude the possibility that they mediate the crosstalk between root and nodule development in soybean.

In addition to gene duplication, the functions of *TIR1* and *AFB3* genes are also regulated at various levels. We found that there was an apparent difference in transcriptional regulation of *TIR1* and *AFB3* genes in response to auxin between Arabidopsis and soybean. Unlike Arabidopsis *TIR1* and *AFB3* genes are not responsive to auxin (Parry *et al.*, 2009), the *GmTIR1* and *GmAFB3* genes are induced by auxin 2,4-D in soybean roots (Fig. 4). The difference in auxin responsiveness between Arabidopsis and soybean receptor genes appears mainly due to the distinction between their promoters; that is, the existence of the auxin-responsive *cis* regulatory elements in the promoters of the soybean auxin receptor genes (Fig. S15). Within 2-kb regions of Arabidopsis *TIR1* and *AFB3* promoters, there were no auxin response-related *cis* elements (Fig. S15a,d). Interestingly, we found several auxin-responsive elements and/or auxin response

factor binding sites in the promoters of *GmTIR1A*, *GmTIR1C* and *GmAFB3A* (Fig. S15b,c,e). In particular, *GmTIR1C* promoter contains both auxin-responsive elements and auxin response factor binding sites (Fig. S15c) (Xu *et al.*, 1997). Transcriptional responsiveness of the *GmTIR1* and *GmAFB3* genes to auxin suggest the presence of feedback regulatory loop acting through these auxin receptor genes, thereby adding another layer of regulation for auxin receptor-mediated nodulation and growth in soybean. Thus, it is apparent that transcriptional regulation of auxin receptor genes has diverged significantly between soybean and *Arabidopsis* during evolution, which may be required for the complex developmental traits including root nodule development in soybean.

Previous data on auxin-inducible gene expression (e.g. *DR5pro::GUS* activity) showed that auxin activity is restricted mainly to nodule periphery in the mature nodules, but not in nitrogen (N)-fixation zones during determinate nodule development (Takanashi *et al.*, 2011; Suzaki *et al.*, 2012; Turner *et al.*, 2013). This observation suggests that auxin response also takes place in these regions, although auxin response as measured by auxin-responsive marker genes is not detected in the infection and N-fixation zones (Turner *et al.*, 2013). This makes sense because the growth of determinate nodules is due largely to plant cell division and expansion, which is auxin's primary role (Kong *et al.*, 2013). It is worthy of note that majority of *GmTIR1/AFB3* genes were highly expressed in meristematic tissues of roots and/or lateral roots (Fig. S5) or the cells/tissues in nodule primordia and developing nodules (Fig. 2). The cell/tissue-specific expression patterns of these *GmTIR1/AFB3* genes imply that the *GmTIR1/AFB3*-mediated auxin signaling and auxin responses of the cells/tissues are required for the development of determinate nodules. The fact that knockdown or overexpression of *GmTIR1/AFB3* genes substantially reduced or increased the nodule number (Figs 1, 3) supports this conclusion. The positive correlation between the concentrations of auxin of infected roots and nodule number may also be conserved in nodule development. In *Lotus japonicum*, the supernodulation mutant *har1* has many more sites that accumulate auxin than the wild-type (Suzaki *et al.*, 2012). In addition to the role of auxin in nodule organogenesis, a recent study of root hair infectome showed that auxin and the auxin signaling also modulate rhizobial infection in *Medicago truncatula* (Breakspear *et al.*, 2014). In the present study we provide direct evidence for the involvement of auxin signaling in rhizobial infection because knockdown of *GmTIR1/AFB3* genes reduced the number of curled root hairs in response to rhizobial infection (Fig. 1a–d). The results suggest that the *GmTIR1/AFB3* gene-mediated auxin signaling also modulates nodulation through affecting the initial step of rhizobial infection. Because the ratio of auxin/cytokinin determines the cell fate during development, it is conceivable that activation or attenuation of auxin signaling by *GmTIR1/AFB3* may affect the balance between cell responses to cytokinin and auxin, thereby changing cell fates of plants.

Previous studies have shown that rhizobia also are able to synthesize auxin, and rhizobial auxin is required for nodule development in both determinate and indeterminate nodules (Hunter, 1987; Pii *et al.*, 2007). The activation of auxin response in the N-

fixation zone of developing nodules could be stimulated by the auxin from host cells, or by rhizobia-derived auxin. Inoculation with *Bradyrhizobium* mutants deficient in auxin synthesis results in reduced number of nodules in soybean (Fukuhara *et al.*, 1994), whereas inoculation with an IAA-overproducing *Sinorhizobium melioli* strain increased nodule numbers in *M. truncatula* (Pii *et al.*, 2007). Thus, auxin signaling also plays an important role in the growth of nodules. This conclusion is supported by the results of Breakspear *et al.* (2014), which showed that *GH3-1*, *SAURI* and *ARF16a* are also expressed in the infection zone of the growing nodules in *M. truncatula* (Breakspear *et al.*, 2014). These results demonstrated that the regulatory role of auxin in the growth of both determinate and indeterminate nodules is conserved. In *M. truncatula*, *GH3-1*, *SAURI* and *ARF16a* expression are restricted mainly to the meristem zone of mature nodules (Breakspear *et al.*, 2014). However, *GmTIR1C* is still expressed in the N-fixation zone upon nodule maturation (Fig. 2k). Because *GH3-1*, *SAURI* and *ARF16a* are downstream effectors in auxin signaling, we speculated that distinct auxin signaling pathways may participate in the functionality of N-fixing nodules.

It is well known that auxin receptor genes *TIR1* and *AFB3* are also regulated at the post-transcriptional level by miR393 in land plants, such as *Arabidopsis* and rice (Xia *et al.*, 2012; Iglesias *et al.*, 2014). Here, we provide evidence that miR393 directly represses expression of *GmTIR1* and *GmAFB3* during soybean nodulation (Figs 6, S9, S13). We demonstrated that miR393d negatively regulates rhizobial infection and nodule development through cleaving the target gene *GmTIR1C* because overexpression of the mutated version of *GmTIR1C* that cannot be cleaved by miR393 resulted in a more severe nodule phenotype than overexpression of the normal *GmTIR1C1* (Figs 7, 8). The effects of miR393 on rhizobial infection and nodule development seem not to be in agreement with the study by Turner *et al.* (2013), showing that miR393(a) do not mediate the development of determinate nodules. This may be due to the different roles of individual miR393 in the regulation of the distinct target genes. Apparently, miR393 members showed different levels of expression during rhizobial infection and nodule development. It is, therefore, possible that given the low expression level of miR393d in the root hairs and cortical cells, the N-fixation zone can relieve the repression of the target genes, allowing activation of auxin signaling and subsequent rhizobial infection, nodule formation and growth. Because there are four more miR393 family members showing similar expression pattern to miR393d during nodulation, we do not exclude the possibility that they are functionally redundant in nodule development.

Because the soybean miR393 and auxin receptors families have multiple members, the regulation of auxin receptors by miR393 is more complicated. Although 5' RACE and transient coexpression of miR393 and the target genes in *N. benthamiana* leaves showed that *GmTIR1* and *GmAFB3* mRNAs were repressed by miR393, each target gene is cleaved precisely by the members of miR393 in soybean. For example, overexpression of miR393d in the composite soybean plants effectively reduced the transcript levels of the *GmTIR1C* and *GmAFB3A* but not the *GmTIR1A*

(Fig. 8). This phenomenon was also observed in the report by Turner *et al.* (2013). However, when the miR393 family members were knocked down by miRNA target mimic technology, expression of all the tested genes (the *GmTIR1C*, *GmAFB3A* and *GmTIR1A*) increased, suggesting that the *GmTIR1A* is targeted by other miR393 family member but not miR393d (Fig. 8). In addition, it was shown previously that *Arabidopsis* miR393 initiated the biogenesis of secondary siRNAs from the transcripts of *TIR1/AFB2* genes, which in turn enhance the repression effect on the target genes by guiding the cleavage of their mRNAs (Si-Ammour *et al.*, 2011). However, in the present study, we did not detect any other cleaved products from the target transcripts in addition to the products at the specific cleavage site between the 10th to 11th nucleotides from the 5' end of miR393, indicating that no siRNAs are produced by the interaction between miR393 and their targets in soybean. This may also explain why overexpression of miR393d does not result in the severe reduction of its target genes.

Taken together, the available data have demonstrated that activation of auxin signaling is required for each step of nodulation in soybean. However, the mechanisms underlying the auxin-mediated infection of rhizobia, nodule primordia formation and nodule growth are complex, and far from being fully investigated and understood. Nevertheless, our finding provides new insight into deciphering this extremely complex developmental process.

Acknowledgements

We thank members of Xia Li's laboratory for their support and constructive suggestions and comments on the work. We are grateful to Dr Kan Wang at Iowa State University for giving us the pTF101.1 vector. We also thank Dr Wenxin Chen at China Agricultural University for kindly providing us the *B. japonicum* strain USDA 110. This study was funded by NSFC (31230050 and 30971797) and the Ministry of Agriculture of the People's Republic of China (2009ZX08009-132B, 2014ZX0800929B). This study was also supported by The Huazhong Agricultural University Scientific & Technological Self-Innovation Foundation (Program no. 2015RC014). This work was also supported by Youth Innovation Promotion Association, Chinese Academy of Sciences, PR China.

Author contributions

X.L. designed the research; Z.C., Y.W., L.Z., Y.T., L.C., Z.S. and I.U. performed the experiments and data analyses; and X.L. and Z.C. wrote the manuscript.

References

- Breakspear A, Liu C, Roy S, Stacey N, Rogers C, Trick M, Morieri G, Mysore KS, Wen J, Oldroyd GE *et al.* 2014. The root hair "infectome" of *Medicago truncatula* uncovers changes in cell cycle genes and reveals a requirement for auxin signaling in rhizobial infection. *Plant Cell* 26: 4680–4701.
- Desbrosses GJ, Stougaard J. 2011. Root nodulation: a paradigm for how plant-microbe symbiosis influences host developmental pathways. *Cell Host & Microbe* 10: 348–358.
- Downie JA. 2014. Legume nodulation. *Current Biology* 24: R184–R190.
- Ferguson BJ, Indrasumunar A, Hayashi S, Lin MH, Lin YH, Reid DE, Gresshoff PM. 2010. Molecular analysis of legume nodule development and autoregulation. *Journal of Integrative Plant Biology* 52: 61–76.
- Fukuhara H, Minakawa Y, Akao S, Minamisawa K. 1994. The involvement of indole-3-acetic acid produced by *Bradyrhizobium elkanii* in nodule formation. *Plant and Cell Physiology* 35: 1261–1265.
- Held M, Hou H, Miri M, Huynh C, Ross L, Hossain MS, Sato S, Tabata S, Perry J, Wang TL *et al.* 2014. *Lotus japonicus* cytokinin receptors work partially redundantly to mediate nodule formation. *Plant Cell* 26: 678–694.
- Hirsch AM, Bhuvanawari TV, Torrey JG, Bisseling T. 1989. Early nodulin genes are induced in alfalfa root outgrowths elicited by auxin transport inhibitors. *Proceedings of the National Academy of Sciences, USA* 86: 1244–1248.
- Hunter WJ. 1987. Influence of 5-methyltryptophan-resistant *Bradyrhizobium japonicum* on soybean root nodule indole-3-acetic acid content. *Applied and Environmental Microbiology* 53: 1051–1055.
- Huo X, Schnabel E, Hughes K, Frugoli J. 2006. RNAi phenotypes and the localization of a protein:GUS fusion imply a role for *Medicago truncatula* PIN genes in nodulation. *Journal of Plant Growth Regulation* 25: 156–165.
- Iglesias MJ, Terrile MC, Windels D, Lombardo MC, Bartoli CG, Vazquez F, Estelle M, Casalogue CA. 2014. miR393 regulation of auxin signaling and redox-related components during acclimation to salinity in *Arabidopsis*. *PLoS ONE* 9: e107678.
- Jian B, Hou W, Wu C, Liu B, Liu W, Song S, Bi Y, Han T. 2009. *Agrobacterium rhizogenes*-mediated transformation of *Superroot*-derived *Lotus corniculatus* plants: a valuable tool for functional genomics. *BMC Plant Biology* 9: 78.
- Jian B, Liu B, Bi Y, Hou W, Wu C, Han T. 2008. Validation of internal control for gene expression study in soybean by quantitative real-time PCR. *BMC Molecular Biology* 9: 59.
- Kereszt A, Li D, Indrasumunar A, Nguyen CD, Nontachaiyapoom S, Kinkema M, Gresshoff PM. 2007. *Agrobacterium rhizogenes*-mediated transformation of soybean to study root biology. *Nature Protocols* 2: 948–952.
- Kong Y, Zhu Y, Gao C, She W, Lin W, Chen Y, Han N, Bian H, Zhu M, Wang J. 2013. Tissue-specific expression of *SMALL AUXIN UP RNA41* differentially regulates cell expansion and root meristem patterning in *Arabidopsis*. *Plant and Cell Physiology* 54: 609–621.
- Mao G, Turner M, Yu O, Subramanian S. 2013. miR393 and miR164 influence indeterminate but not determinate nodule development. *Plant Signaling & Behavior* 8: e26753.
- Mathesius U, Schlaman HR, Spaik HP, Of Sautter C, Rolfe BG, Djordjevic MA. 1998. Auxin transport inhibition precedes root nodule formation in white clover roots and is regulated by flavonoids and derivatives of chitin oligosaccharides. *Plant Journal* 14: 23–34.
- van Noorden GE, Kerim T, Goffard N, Wiblin R, Pellerone FI, Rolfe BG, Mathesius U. 2007. Overlap of proteome changes in *Medicago truncatula* in response to auxin and *Sinorhizobium meliloti*. *Plant Physiology* 144: 1115–1131.
- van Noorden GE, Ross JJ, Reid JB, Rolfe BG, Mathesius U. 2006. Defective long-distance auxin transport regulation in the *Medicago truncatula* *super numeric nodules* mutant. *Plant Physiology* 140: 1494–1506.
- Pacios-Bras C, Schlaman HR, Boot K, Admiraal P, Langerak JM, Stougaard J, Spaik HP. 2003. Auxin distribution in *Lotus japonicus* during root nodule development. *Plant Molecular Biology* 52: 1169–1180.
- Parry G, Calderon-Villalobos L, Prigge M, Peret B, Dharmasiri S, Itoh H, Lechner E, Gray W, Bennett M, Estelle M. 2009. Complex regulation of the TIR1/AFB family of auxin receptors. *Proceedings of the National Academy of Sciences, USA* 106: 22540–22545.
- Peer WA. 2013. From perception to attenuation: auxin signalling and responses. *Current Opinion in Plant Biology* 16: 561–568.
- Pii Y, Crimi M, Cremonese G, Spena A, Pandolfini T. 2007. Auxin and nitric oxide control indeterminate nodule formation. *BMC Plant Biology* 7: 21.
- Plet J, Wasson A, Ariel F, Le Signor C, Baker D, Mathesius U, Crespi M, Frugier F. 2011. MtCRE1-dependent cytokinin signaling integrates bacterial and plant cues to coordinate symbiotic nodule organogenesis in *Medicago truncatula*. *Plant Journal* 65: 622–633.
- Reid DE, Ferguson BJ, Gresshoff PM. 2010. Inoculation- and nitrate-induced CLE peptides of soybean control NARK-dependent nodule formation. *Molecular Plant-Microbe Interactions* 24: 606–618.

- Roy S, Robson FC, Lilley JL, Liu C, Cheng X, Wen J, Bone C, Walker S, Sun J, Cousins D *et al.* 2017. MtLAX2, a functional homologue of the auxin importer AtAUX1, is required for nodule organogenesis. *Plant Physiology* 174: 326–338.
- Sańko-Sawczenko I, Łotocka B, Czarnocka W. 2016. Expression analysis of *PIN* genes in root tips and nodules of *Medicago truncatula*. *International Journal of Molecular Sciences* 17: 1197.
- Si-Ammour A, Windels D, Arn-Bouidoires E, Kutter C, Ailhas J, Meins F Jr, Vazquez F. 2011. miR393 and secondary siRNAs regulate expression of the *TIR1/AFB2* auxin receptor clade and auxin-related development of Arabidopsis leaves. *Plant Physiology* 157: 683–691.
- Streeter JG. 1985. Nitrate inhibition of legume nodule growth and activity: II. Short term studies with high nitrate supply. *Plant Physiology* 77: 325–328.
- Subramanian S, Hu X, Lu G, Odelland JT, Yu O. 2004. The promoters of two isoflavone synthase genes respond differentially to nodulation and defense signals in transgenic soybean roots. *Plant Molecular Biology* 54: 623–639.
- Suzaki T, Yano K, Ito M, Umehara Y, Suganuma N, Kawaguchi M. 2012. Positive and negative regulation of cortical cell division during root nodule development in *Lotus japonicus* is accompanied by auxin response. *Development* 139: 3997–4006.
- Takanashi K, Sugiyama A, Yazaki K. 2011. Involvement of auxin distribution in root nodule development of *Lotus japonicus*. *Planta* 234: 73–81.
- Tan X, Calderon-Villalobos LI, Sharon M, Zheng C, Robinson CV, Estelle M, Zheng N. 2007. Mechanism of auxin perception by the TIR1 ubiquitin ligase. *Nature* 446: 640–645.
- Todesco M, Rubio-Somoza I, Paz-Ares J, Weigel D. 2010. A collection of target mimics for comprehensive analysis of microRNA function in *Arabidopsis thaliana*. *PLoS Genetics* 6: e1001031.
- Turner M, Nizampatnam NR, Baron M, Coppin S, Damodaran S, Adhikari S, Arunachalam SP, Yu O, Subramanian S. 2013. Ectopic expression of miR160 results in auxin hypersensitivity, cytokinin hyposensitivity, and inhibition of symbiotic nodule development in soybean. *Plant Physiology* 162: 2042–2055.
- Vidal EA, Moyano TC, Riveras E, Contreras-López O, Gutiérrez RA. 2013. Systems approaches map regulatory networks downstream of the auxin receptor AFB3 in the nitrate response of *Arabidopsis thaliana* roots. *Proceedings of the National Academy of Sciences, USA* 110: 12 840–12 845.
- Wang Y, Li P, Cao X, Wang X, Zhang A, Li X. 2009. Identification and expression analysis of miRNAs from nitrogen-fixing soybean nodules. *Biochemical and Biophysical Research Communications* 378: 799–803.
- Wang Y, Li K, Chen L, Zou Y, Liu H, Tian Y, Li D, Wang R, Zhao F, Ferguson BJ *et al.* 2015. microRNA167-directed regulation of the auxin response factors, GmARF8a and GmARF8b, is required for soybean (*Glycine max* L.) nodulation and lateral root development. *Plant Physiology* 168: 984–999.
- Wasson AP, Pellerone FI, Mathesius U. 2006. Silencing the flavonoid pathway in *Medicago truncatula* inhibits root nodule formation and prevents auxin transport regulation by rhizobia. *Plant Cell* 18: 1617–1629.
- Xia K, Wang R, Ou X, Fang Z, Tian C, Duan J, Wang Y, Zhang M. 2012. *OsTIR1* and *OsAFB2* downregulation via *OsmiR393* overexpression leads to more tillers, early flowering and less tolerance to salt and drought in rice. *PLoS ONE* 7: e30039.
- Xu N, Hagen G, Guilfoyle T. 1997. Multiple auxin response modules in the soybean *SAUR 15A* promoter. *Plant Science* 126: 193–201.
- Yan Z, Hossain MS, Arikat S, Valdés-López O, Zhai J, Wang J, Libault M, Ji T, Qiu L, Meyers BC *et al.* 2015. Identification of microRNAs and their mRNA targets during soybean nodule development: functional analysis of the role of miR393j-3p in soybean nodulation. *New Phytologist* 207: 748–759.
- Fig. S1** The orthologs of Arabidopsis auxin receptor *AtTIR1/AFB3* family genes in soybean genome and the structure of the gene.
- Fig. S2** The protein sequence alignment between soybean and Arabidopsis TIR1/AFB3.
- Fig. S3** The phylogenetic analysis of auxin receptors GmTIR1 and GmAFB3 family proteins in soybean.
- Fig. S4** The integrative orthology analysis among the *AtTIR1/AFB* and *GmTIR1/AFB* family members.
- Fig. S5** The histochemical chemical analysis of the *GmTIR1/GmAFB* genes in the noninoculated roots.
- Fig. S6** The expression patterns of *GmTIR1A*, *GmTIR1C* and *GmAFB3A* during nodulation.
- Fig. S7** The identification of transgenic hairy roots overexpressing *GmTIR1A*, *GmTIR1C* and *GmAFB3A*.
- Fig. S8** *GmTIR1A*, *GmTIR1C* and *GmAFB3A* are induced by 2, 4-D treatment in soybean roots.
- Fig. S9** *GmTIR1A*, *GmTIR1C* and *GmAFB3A* mRNAs are cleaved by miR393.
- Fig. S10** Expression analysis of the soybean miR393 family genes.
- Fig. S11** The subcellular localization of GmTIR1A, GmTIR1C and GmAFB3A.
- Fig. S12** The four point mutations of *GmTIR1C*.
- Fig. S13** *GmTIR1A* and *GmAFB3A* are repressed by miR393d.
- Fig. S14** Diagram of *MIM393* depicting knock-down of miR393 expression.
- Fig. S15** The promoter *cis*-element analysis of Arabidopsis *TIR1/AFB3* and *GmTIR1/GmAFB3* genes.
- Table S1** The primers used in the study
- Table S2** The identity of sequences between *AtTIR1/AFB3* and *GmTIR1/AFB3*
- Table S3** The mature sequences of miR393 family members and their chromosome locations in soybean

Supporting Information

Additional Supporting Information may be found online in the Supporting Information tab for this article:

Fig. S1 The orthologs of Arabidopsis auxin receptor *AtTIR1/AFB3* family genes in soybean genome and the structure of the gene.

Please note: Wiley Blackwell are not responsible for the content or functionality of any Supporting Information supplied by the authors. Any queries (other than missing material) should be directed to the *New Phytologist* Central Office.